nature neuroscience

Leptin signaling in astrocytes regulates hypothalamic neuronal circuits and feeding

Jae Geun Kim[1], Shigetomo Suyama[1], Marco Koch[1,2], Sungho Jin[1], Pilar Argente-Arizon[3], Jesús Argente[3], Zhong-Wu Liu[1], Marcelo R Zimmer[1], Jin Kwon Jeong[1,4], Klara Szigeti-Buck[1], Yuanqing Gao[5], Cristina Garcia-Caceres[5], Chun-Xia Yi[5], Natalina Salmaso[6], Flora M Vaccarino[6,7], Julie Chowen[3], Sabrina Diano[1,4,7], Marcelo O Dietrich[1], Matthias H Tschöp[5] & Tamas L Horvath[1,4,7]

We found that leptin receptors were expressed in hypothalamic astrocytes and that their conditional deletion led to altered glial morphology and synaptic inputs onto hypothalamic neurons involved in feeding control. Leptin-regulated feeding was diminished, whereas feeding after fasting or ghrelin administration was elevated in mice with astrocyte-specific leptin receptor deficiency. These data reveal an active role of glial cells in hypothalamic synaptic remodeling and control of feeding by leptin.

Astrocytes are the most abundant cells in the CNS, yet they have often been relegated to a less than prominent role in the control of complex brain functions supported by neuronal circuits[1,2]. The regulation of food intake and energy expenditure is tightly linked to the synaptic plasticity of hypothalamic neural circuits[3,4], processes in which glial cells have also been implicated[5,6]. It has not yet been explored whether this involvement of glia is secondary or has an active role in the promotion of these processes initiated by leptin[7].

Previously, the long form of leptin receptors (*Lepr*) was located in astrocytes via immunocytochemistry[8,9]. However, because of questions regarding antibody specificity, it remains controversial whether astrocytes express functional *Lepr*. We found immunolabeling of glial fibrillary acidic protein (GFAP) in a subset of *Lepr*-driven EGFP-expressing cells (**Supplementary Fig. 1**). *Lepr* mRNA was detected from translating ribosomes of astrocytes (**Supplementary Fig. 1**). Finally, we found that mRNA of *Lepr* was expressed in purified mouse hypothalamic astrocytes using astrocyte primary culture (**Supplementary Fig. 2**).

To test the role of the long form of leptin receptors in glial cells, we generated a genetic mouse model in which leptin receptors are time-specifically ablated in astrocytes. Because glial cells are the progenitor cells for neurogenesis during brain development[10], we used a tamoxifen-inducible *Cre-ERT2* system to allow cell- and time-specific knockout of leptin receptor in adult astrocytes (**Supplementary Fig. 2**). To assess whether functional Cre protein was restricted to astrocytes and induced by tamoxifen injection, we crossed GFAP-CreERT2 mice with tdTomato-loxP reporter mice, which express red fluorescent protein. We confirmed successful Cre-mediated recombination in GFAP-positive cells by detecting tdTomato-positive cells after injection of tamoxifen (**Supplementary Fig. 3**). This recombination was found to be specific to astrocytes, as the tdTomato-positive cells did not express Iba-1 (a marker for microglia) or NeuN (a marker for neurons) (**Supplementary Fig. 3**). In addition, we combined *in situ* hybridization with immunohistochemistry to validate the selective loss of functional leptin receptors from GFAP-positive cells in GFAP-Cre transgenic mice that are homozygous for a *loxP*-flanked *Lepr* allele (**Fig. 1a** and **Supplementary Fig. 1**). We further confirmed the deletion of leptin receptor exon 17 in astrocyte primary cells of *Gfap-Lepr*$^{-/-}$ mice by reverse transcription (RT)-PCR (**Supplementary Fig. 2**).

Given that we previously found that leptin affects glial morphology[6,11], we first analyzed astrocytes in the arcuate nucleus of mice following leptin receptor knockout (**Fig. 1b**). Astrocyte-specific loss of leptin receptors did not alter the total number of GFAP-positive cells in the hypothalamus (**Fig. 1c**). However, *Gfap-Lepr*$^{-/-}$ mice showed fewer numbers (**Fig. 1d**) and shorter lengths (**Fig. 1e**) of primary astrocytic projections. We also analyzed astrocytes in the hippocampus. Notably, we detected *Lepr* mRNA in the hippocampus (**Supplementary Fig. 4a**), but there were no changes regarding the number and morphology of GFAP-positive cells (**Supplementary Fig. 4b–e**).

Previously, we reported that astrocytic processes are involved in synaptic plasticity of feeding circuits, including those comprising the proopiomelanocortin (POMC) neurons that secrete α-melanocyte stimulating hormone (α-MSH) and AgRP (agouti-related protein) neurons that co-produce neuropeptide Y (NPY) and GABA[5,6]. This led us to evaluate the patterns of glial ensheathment onto the perikaryal membranes of POMC and unlabeled neurons in the arcuate nucleus by electron microscopy. *Gfap-Lepr*$^{-/-}$ mice had lower glial coverage on the perikaryal membranes of POMC (**Fig. 1f** and **Supplementary Fig. 5a**) and unlabeled neurons (**Fig. 1g**) than control mice. We then analyzed glial coverage of POMC and AgRP cells of *Gfap-Lepr*$^{-/-}$ mice using double immunofluorescence: GFAP immonolabeled with red fluorescence in association with green fluorescent protein (GFP)-labeled POMC or AgRP neurons (*Npy-hrGFP* mice were used for the latter; these mice allow visualization of AgRP neurons through coexpression of NPY and AgRP in these cells). We found that direct contacts were lower between astrocytes and either POMC (**Supplementary Fig. 5b**,**c**) or AgRP (**Supplementary Fig. 5d**,**e**) neurons in *Gfap-Lepr*$^{-/-}$ mice relative to control values.

[1]Program in Integrative Cell Signaling and Neurobiology of Metabolism, Section of Comparative Medicine, Yale University School of Medicine, New Haven, Connecticut, USA. [2]Institute of Anatomy, University of Leipzig, Leipzig, Germany. [3]Hospital Infantil Universitario Niño Jesús, Department of Endocrinology, Instituto de Investigación La Princesa and Centro de Investigación Biomédica en Red de la Fisiopatología (CIBER) de Fisiopatología de Obesidad y Nutrición, Instituto de Salud Carlos III, Madrid, Spain. [4]Department of Obstetrics, Gynecology, and Reproductive Sciences, Yale University School of Medicine, New Haven, Connecticut, USA. [5]Institute for Diabetes and Obesity, Helmholtz Zentrum München & Technische Universität München, Germany. [6]Child Study Center, Yale University School of Medicine, New Haven, Connecticut, USA. [7]Department of Neurobiology, Yale University School of Medicine, New Haven, Connecticut, USA. Correspondence should be addressed to T.L.H. (tamas.horvath@yale.edu).

Received 16 February; accepted 24 April; published online 1 June 2014; doi:10.1038/nn.3725

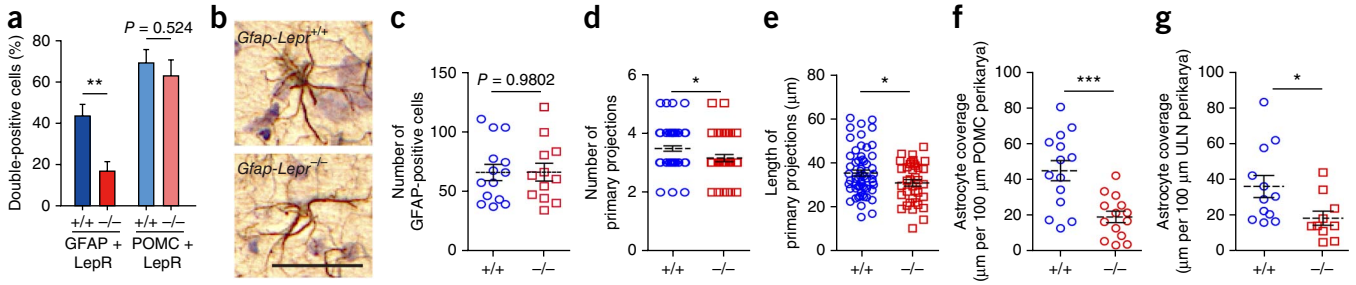

Figure 1 Cell autonomous impairment of leptin receptor (LepR) signaling alters astrocyte morphology and reduces astrocytic coverage onto melanocortin cells. (**a**) Bar graphs show the number of astrocytes or POMC cells expressing *Lepr* mRNA in the Arc (GFAP + LepR, $n = 6$ slices for *Gfap-Lepr*$^{+/+}$ (+/+), $n = 6$ slices for *Gfap-Lepr*$^{-/-}$ (–/–), $P = 0.0041$, $t_{10} = 3.699$; POMC + LepR, $n = 6$ slices for *Gfap-Lepr*$^{+/+}$, $n = 6$ slices for *Gfap-Lepr*$^{-/-}$, $P = 0.524$, $t_{10} = 0.6603$). (**b**) Representative image of GFAP immunolabeling in the Arc of *Gfap-Lepr*$^{+/+}$ and *Gfap-Lepr*$^{-/-}$ mice. Scale bar represents 100 µm. (**c**–**e**) The number of GFAP-positive cells did not differ between *Gfap-Lepr*$^{+/+}$ and *Gfap-Lepr*$^{-/-}$ mice ($n = 14$ slices for *Gfap-Lepr*$^{+/+}$, $n = 12$ slices for *Gfap-Lepr*$^{-/-}$, $P = 0.9802$, $t_{24} = 0.02503$; **c**), but the number of primary projections ($n = 59$ cells for *Gfap-Lepr*$^{+/+}$, $n = 39$ cells for *Gfap-Lepr*$^{-/-}$, $P = 0.0334$, $t_{96} = 2.158$; **d**) and their length ($n = 59$ cells for *Gfap-Lepr*$^{+/+}$, $n = 37$ cells for *Gfap-Lepr*$^{-/-}$, $P = 0.0403$, $t_{94} = 2.079$; **e**) were less in *Gfap-Lepr*$^{-/-}$ mice than in *Gfap-Lepr*$^{+/+}$ mice. (**f**,**g**) POMC cells ($n = 14$ cells for *Gfap-Lepr*$^{+/+}$, $n = 14$ cells for *Gfap-Lepr*$^{-/-}$, $P = 0.0005$, $t_{26} = 3.989$; **f**), and unlabeled neurons (ULN) ($n = 12$ cells for *Gfap-Lepr*$^{+/+}$, $n = 10$ cells for *Gfap-Lepr*$^{-/-}$, $P = 0.0316$, $t_{20} = 1.967$; **g**) in their vicinity, of *Gfap-Lepr*$^{-/-}$ mice had less coverage of their perikaryal membranes by astrocytic processes compared with controls. $^*P < 0.05$, $^{**}P < 0.01$, $^{***}P < 0.001$ versus *Gfap-Lepr*$^{+/+}$. Data are presented as means ± the s.e.m. *P* values for unpaired comparisons were analyzed by two-tailed Student's *t* test.

Next, we assessed whether reduced astrocyte coverage affects synapse number on arcuate nucleus neurons. First, we analyzed synapse number and type by electron microscopy. We found that there were elevated numbers of both symmetric and asymmetric synapses on both POMC (**Fig. 2a**,**b**) and unlabeled neuronal perikarya (**Fig. 2c**) in *Gfap-Lepr*$^{-/-}$ mice relative to controls. Accordingly, we found an elevated frequency of miniature inhibitory postsynaptic currents onto POMC neurons (mIPSCs; **Fig. 2d**), but there was no change in the frequency of miniature excitatory postsynaptic currents onto POMC neurons (mEPSCs) onto POMC cells (**Fig. 2e**). AgRP neurons had an increase in the frequency of both mIPSCs and mEPSCs (**Fig. 2f**,**g**). Taken together, these data indicate that leptin receptor signaling in astrocytes regulates the synaptic input organization of AgRP and POMC cells. We also observed an increase in the amplitudes of both mIPSCs and mEPSCs onto the POMC neurons of *Gfap-Lepr*$^{-/-}$ mice (**Supplementary Fig. 6c**,**d**). On the other hand, there was no alteration in the amplitude of miniature postsynaptic currents onto the AgRP neurons (**Supplementary Fig. 6a**,**b**). These findings suggest that the reduced astrocyte coverage may affect the signaling pathways linked to the postsynaptic receptors of POMC neurons, presumably by buffering trophic factors in the respective synaptic cleft area.

We previously found that the synaptic input organization of the melanocortin system predicts the behavioral output of the melanocortin system in the face of a changing metabolic milieu[3,5,12]. Thus, we next assessed the metabolic phenotype of *Gfap-Lepr*$^{-/-}$ mice and their littermate controls but found them to be normal in phenotypes

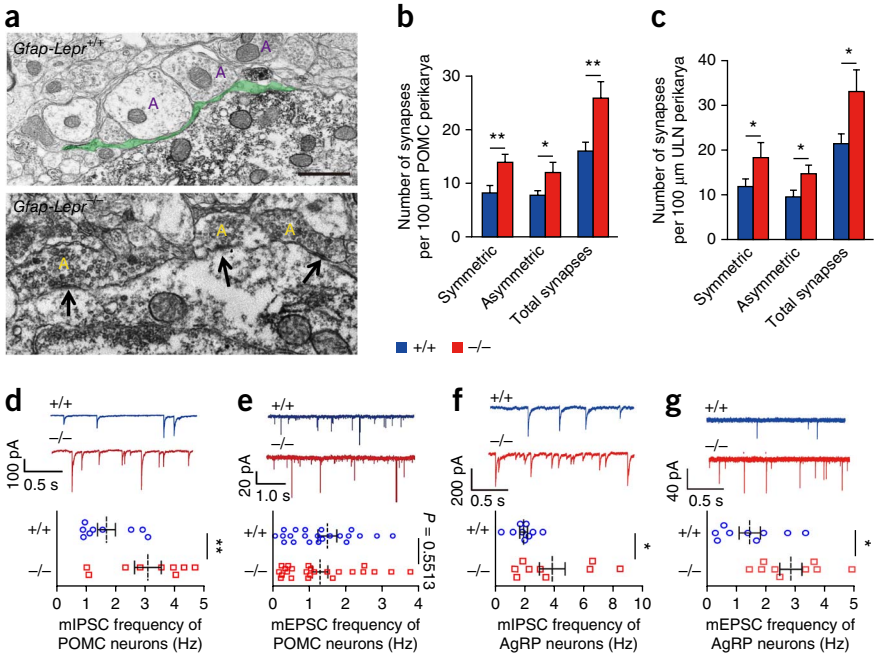

Figure 2 Impaired leptin receptor signaling in astrocytes increases the number of synapses onto POMC and AgRP neurons. (**a**) Representative electron micrograph showing astrocyte coverage (green pseudo-color) and synapses (black arrows) onto POMC-labeled cells. Scale bar represent 1 µm. A, axon. (**b**,**c**) POMC cells ($n = 19$ cells for *Gfap-Lepr*$^{+/+}$ (+/+), $n = 15$ cells for *Gfap-Lepr*$^{-/-}$ (–/–); $P = 0.0097$, $t_{32} = 2.751$ for symmetric; $P = 0.0311$, $t_{32} = 2.255$ for asymmetric; $P = 0.0047$, $t_{32} = 3.039$ for total; **b**), as well as unlabeled neurons (ULN; **c**) ($n = 12$ cells for *Gfap-Lepr*$^{+/+}$, $n = 10$ cells for *Gfap-Lepr*$^{-/-}$; $P = 0.0466$, $t_{20} = 1.763$ for symmetric; $P = 0.0352$, $t_{20} = 2.259$ for asymmetric; $P = 0.0297$, $t_{20} = 2.341$ for total) in their vicinity, of *Gfap-Lepr*$^{-/-}$ mice had elevated numbers of symmetric, asymmetric and, thus, total synapses on their perikaryal membrane compared with controls. (**d**,**e**) POMC neurons (identified by *Pomc*-driven *GFP* labeling) of *Gfap-Lepr*$^{-/-}$ mice had an elevated frequency of mIPSCs ($n = 9$ cells for *Gfap-Lepr*$^{+/+}$, $n = 9$ cells for *Gfap-Lepr*$^{-/-}$, $P = 0.0203$, $t_{16} = 2.576$; **d**), but we found no changes in the frequency of mEPSCs ($n = 23$ cells for *Gfap-Lepr*$^{+/+}$, $n = 25$ cells for *Gfap-Lepr*$^{-/-}$, $P = 0.5513$, $t_{45} = 0.6003$; **e**). (**f**,**g**) AgRP neurons (identified by *NPY*-driven *hrGFP* labeling) of *Gfap-Lepr*$^{-/-}$ mice had an elevated frequency of mIPSCs ($n = 9$ cells for *Gfap-Lepr*$^{+/+}$, $n = 9$ cells for *Gfap-Lepr*$^{-/-}$, $P = 0.0493$, $t_{16} = 2.127$; **f**) and mEPSCs ($n = 9$ cells for *Gfap-Lepr*$^{+/+}$, $n = 9$ cells for *Gfap-Lepr*$^{-/-}$, $P = 0.0164$, $t_{16} = 2.681$; **g**). $^*P < 0.05$, $^{**}P < 0.01$ versus (+/+). Data are presented as means ± the s.e.m. *P* values for unpaired comparisons were analyzed by two-tailed Student's *t* test.

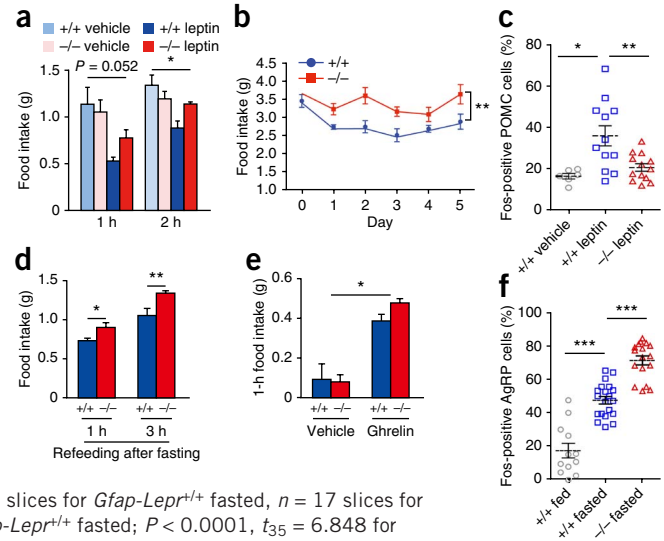

Figure 3 Impairment of leptin receptor signaling in astrocytes blunts leptin-induced anorexia and enhances fasting or ghrelin-induced hyperphagia. (**a**,**b**) *Gfap-Lepr*$^{-/-}$ (–/–) mice showed blunted suppression of feeding in response to leptin administration (**a**: $n = 5$ mice for *Gfap-Lepr*$^{+/+}$ (+/+) + vehicle, *Gfap-Lepr*$^{-/-}$ + vehicle and *Gfap-Lepr*$^{-/-}$ + leptin, $n = 6$ mice for *Gfap-Lepr*$^{+/+}$ + leptin; $P = 0.052$, $F_{1,17} = 4.386$ for 1 h; $P = 0.018$, $F_{1,17} = 6.873$ for 2 h; **b**: $n = 6$ mice per group, $P = 0.0095$, $F_{9,36} = 2.971$). (**c**) Number of Fos-positive POMC cells induced by leptin treatment was reduced in *Gfap-Lepr*$^{-/-}$ mice ($n = 6$ slices for *Gfap-Lepr*$^{+/+}$ + vehicle, $n = 12$ slices for *Gfap-Lepr*$^{+/+}$ + leptin, $n = 13$ slices for *Gfap-Lepr*$^{-/-}$ + leptin; $P = 0.013$, $t_{16} = 2.788$ for *Gfap-Lepr*$^{+/+}$ + vehicle versus *Gfap-Lepr*$^{+/+}$ + leptin; $P = 0.0056$, $t_{23} = 3.055$ for *Gfap-Lepr*$^{+/+}$ + leptin versus *Gfap-Lepr*$^{-/-}$ + leptin). (**d**–**f**) *Gfap-Lepr*$^{-/-}$ mice showed increased feeding after fasting or ghrelin administration (**d**: $n = 6$ mice for *Gfap-Lepr*$^{+/+}$, $n = 7$ mice for *Gfap-Lepr*$^{-/-}$; $P = 0.0378$, $t_{11} = 2.361$ for 1 h; $P = 0.0092$, $t_{11} = 3.150$ for 3 h; **e**: $n = 5$ mice for *Gfap-Lepr*$^{+/+}$ + vehicle, $n = 6$ mice for *Gfap-Lepr*$^{-/-}$ + vehicle, $n = 12$ mice for *Gfap-Lepr*$^{+/+}$ + ghrelin, $n = 11$ mice for *Gfap-Lepr*$^{-/-}$ + ghrelin, $P = 0.04$, $F_{1,32} = 4.57$). (**f**) The number of Fos-positive AgRP cells induced by overnight fasting was enhanced in *Gfap-Lepr*$^{-/-}$ mice ($n = 12$ slices for *Gfap-Lepr*$^{+/+}$ fed, $n = 20$ slices for *Gfap-Lepr*$^{+/+}$ fasted, $n = 17$ slices for *Gfap-Lepr*$^{-/-}$ fasted; $P < 0.0001$, $t_{30} = 6.721$ for *Gfap-Lepr*$^{+/+}$ fed versus *Gfap-Lepr*$^{+/+}$ fasted; $P < 0.0001$, $t_{35} = 6.848$ for *Gfap-Lepr*$^{+/+}$ fasted versus *Gfap-Lepr*$^{-/-}$ fasted). White arrows indicate double-labeled cells. $^{*}P < 0.05$, $^{**}P < 0.01$, $^{***}P < 0.001$ versus (+/+), leptin or fasted. Data are presented as means ± the s.e.m. *P* values for unpaired comparisons were analyzed by two-tailed Student's *t* test. Two-way ANOVA was performed to detect significant interaction between genotype and treatment (leptin or ghrelin). Two-way repeated-measures ANOVA was performed to detect significant interaction between genotype and time (multiple injections of leptin).

of 3-month-old *Gfap-Lepr*$^{-/-}$ mice under standard feeding conditions (**Supplementary Fig. 7a–h**). However, the effects of both single and multiple injections of leptin to suppress feeding were diminished in *Gfap-Lepr*$^{-/-}$ mice relative to controls (**Fig. 3a**,**b**). Consistent with these results, leptin-stimulated Fos activity was attenuated in the *Gfap-Lepr*$^{-/-}$ mice (**Fig. 3c** and **Supplementary Fig. 8a**). These findings are consistent with the observed increase in the number of inhibitory inputs onto the POMC neurons in these mice, as it has been shown that leptin exerts its effect on POMC neurons, at least in part, by the suppression of their inhibitory inputs[13,14]. The effect of the selective knockout of *Lepr* in astrocytes on mIPSCs (but not on mEPSCs) recapitulated the effects of leptin that we previously observed in *Lep*$^{ob/ob}$ mice. However, the lack of a measurable effect of leptin on mEPSCs of POMC cells was not reflected in morphological alterations regarding putative excitatory inputs. These discrepancies may be a result of the fact that leptin signaling is more broadly affected in *Lep*$^{ob/ob}$ mice, but they also highlight the idea that the interrogation of circuit integrity and function cannot be reliably asserted by a single approach.

Next, we determined the responses of *Gfap-Lepr*$^{-/-}$ mice to fasting or ghrelin, a gut hormone that is elevated during negative energy balance and that promotes feeding behavior[15,16]. Fasting-induced hyperphagia was enhanced in these mice compared with controls (**Fig. 3d**). *Gfap-Lepr*$^{-/-}$ mice also showed elevated ghrelin-induced food intake (**Fig. 3e**). Consistent with these findings, AgRP neurons of *Gfap-Lepr*$^{-/-}$ mice exhibited an increased number of Fos-expressing nuclei in response to fasting than controls (**Fig. 3f** and **Supplementary Fig. 8b**). These observations are consistent with the findings that food deprivation or ghrelin administration elevates AgRP neuronal activity, at least in part, by mediation of presynaptic excitatory inputs[17], which we found to be controlled by astrocytes.

Collectively, we found that that leptin receptor signaling in astrocytes has a previously underappreciated active role at the arcuate nucleus interface between afferent hormones, hypothalamic synaptic adaptations and strength, and CNS control of feeding. The extent to which these processes may be involved in the development of obesity in response to overnutrition and the identity of the intercellular signaling modalities that enables glial cells to alter synaptology need to be determined.

METHODS

Methods and any associated references are available in the online version of the paper.

Note: Any Supplementary Information and Source Data files are available in the online version of the paper.

ACKNOWLEDGMENTS

This work was supported by the US National Institutes of Health (DP1 DK098058, R01AG040236, P01NS062686 and R01 DK097566), the American Diabetes Association, the Helmholtz Society (ICEMED) and the Klarmann Family Foundation.

AUTHOR CONTRIBUTIONS

J.G.K., M.O.D. and T.L.H. designed the study. J.G.K., M.H.T. and T.L.H. interpreted the results. J.G.K. and S.J. performed the experiments and analyzed the data. M.K. and K.S.-B. contributed to **Figures 1h**,**j** and **2a–c**. J.K.J. and S.D. contributed to **Figure 1c**. S.S. and Z.-W.L. contributed to **Figure 2d–g** and **Supplementary Figure 6**. M.R.Z., N.S. and F.M.V. contributed to **Supplementary Figures 1** and **4a**. P.A.-A., J.C. and J.A. contributed to **Supplementary Figure 2b**. Y.G., C.G.-C. and C.-X.Y. contributed to the generation of the animal model. J.G.K. and T.L.H. wrote the paper with input from the other authors.

COMPETING FINANCIAL INTERESTS

The authors declare no competing financial interests.

1. Bélanger, M., Allaman, I. & Magistretti, P.J. *Cell Metab.* **14**, 724–738 (2011).
2. Allaman, I., Belanger, M. & Magistretti, P.J. *Trends Neurosci.* **34**, 76–87 (2011).
3. West, M.J. & Gundersen, H.J. *J. Comp. Neurol.* **296**, 1–22 (1990).
4. Diano, S., Naftolin, F. & Horvath, T.L. *J. Neuroendocrinol.* **10**, 239–247 (1998).
5. Horvath, T.L. *et al. Proc. Natl. Acad. Sci. USA* **107**, 14875–14880 (2010).
6. Fuente-Martín, E. *et al. J. Clin. Invest.* **122**, 3900–3913 (2012).
7. Sholl, D.A. *J. Anat.* **93**, 143–158 (1959).
8. Hsuchou, H., Pan, W., Barnes, M.J. & Kastin, A.J. *Peptides* **30**, 2275–2280 (2009).
9. Hsuchou, H. *et al. Brain* **132**, 889–902 (2009).
10. Ganat, Y.M. *et al. J. Neurosci.* **26**, 8609–8621 (2006).
11. García-Cáceres, C. *et al. Endocrinology* **152**, 1809–1818 (2011).
12. Gao, Q. & Horvath, T.L. *Annu. Rev. Neurosci.* **30**, 367–398 (2007).
13. Cowley, M.A. *et al. Nature* **411**, 480–484 (2001).
14. Vong, L. *et al. Neuron* **71**, 142–154 (2011).
15. Cowley, M.A. *et al. Neuron* **37**, 649–661 (2003).
16. Andrews, Z.B. *et al. Nature* **454**, 846–851 (2008).
17. Yang, Y., Atasoy, D., Su, H.H. & Sternson, S.M. *Cell* **146**, 992–1003 (2011).

ONLINE METHODS

Animal. Two transgenic mice lines (GFAP-CreERT2 and *Lepr*$^{loxP/loxP}$ mice) were obtained and crossed. GFAP-CreERT2 mice[10], which are inducible transgenic mice under control of human *GFAP* promoter and estrogen (C57BL/6J background, generated by F.M. Vaccarino, Yale University School of Medicine) were mated with *Lepr*$^{loxP/loxP}$ mice[18] (generated by S. Chua, Albert Einstein College of Medicine), and breeding cages were maintained by mating *Lepr*$^{loxP/loxP}$ and *Lepr*$^{loxP/loxP}$; GFAP-CreERT2 mice. To excise *loxP* sites by Cre recombination, 5-week-old male mice were administrated tamoxifen twice a day (100 mg per kg of body weight, intraperitoneal) for 5 d. Tamoxifen (Sigma-Aldrich) was dissolved in sunflower oil at a final concentration of 10 mg ml^{-1} at 37 °C, and then filter sterilized and stored for up to 7 d at 4 °C in the dark. All control groups were tamoxifen-injected littermate control mice (*Lepr*$^{loxP/loxP}$). Genotyping was done by PCR using primer sets binding to *Cre* (Cre-1084, 5′-GCG GTC TGG CAG TAA AAA CTA TC-3′; Cre-1085, 5′-GTG AAA CAG CAT TGC TGT CAC TT-3′; Cre-42, 5′-CTA GGC CAC AGA ATT GAA AGA TCT-3′, Cre-43, 5′-GTA GGT GGA AAT TCT AGC ATC ATC C-3′) and crossing the *loxP* site (65A, 5′-AGA ATG AAA AAG TTG TTT TGG GA-3′; 105, 5′-ACA GGC TTG AGA ACA TGA ACA C-3′; 106, 5′-GTC TGA TTT GAT AGA TGG TCT T-3′). To generate POMC or NPY neuron-specific GFP-labeled mice, *Lepr*$^{loxP/loxP}$; GFAP-CreERT2 mice were mated with transgenic mice expressing GFP in POMC neurons (#008322, Jackson Laboratories) or hrGFP in NPY neurons (#006417, Jackson Laboratories). To confirm specific Cre-mediated recombination in GFAP-positive cell, inducible *Cre* expression was screened by mouse line (GFAP-CreERT2 + *Gt(ROSA)26Sor*$^{tm14(CAG-tdTomato)Hze}$ (#007914, Jackson Laboratories)) with injection of tamoxifen (100 mg per kg, intraperitoneal) twice a day for 5 consecutive days. To identify expression of leptin receptor in astrocyte, we used a mouse model[19] (*Lepr-Cre* + Rosa26 ^{EGFP}; obtained from M.G. Myers Jr., University of Michigan) that expresses EGFP in leptin receptor–positive cells. All animals were kept in temperature- and humidity-controlled rooms on a 12-h:12-h light:dark cycle, with lights on from 7:00 a.m. to 7:00 p.m. Mice were group housed (3–5 mice per cage) and food and water were provided *ad libitum*. All procedures were approved by the Institutional Animal Care and Use Committee of Yale University.

Food intake measurement. All mice used in these studies were 2-month-old males and were individually caged 5 d before the start of feeding studies to allow the animals to acclimatize to their new environment. For the fasting-induced feeding behavior, 1- and 3-h rebounded food intake were measured after 18-h food deprivation (beginning at 2 h before the dark cycle). For the ghrelin-induced feeding, mice received ghrelin (3 mg per kg, intraperitoneal) at the early light cycle (ZT 3). Food pellets were weighted and added to the mouse cage 30 min after ghrelin injection and 1-h food intake was measured. To determine the leptin response on feeding behavior, mice were food deprived for overnight (18 h) and then received leptin (3 mg per kg, intraperitoneal) 2 h after the dark cycle (ZT 14). 1- and 2-h food intake were measured 30 min after leptin injection. To determine the effect of repetitive injection of leptin on daily food intake, food intake was measured every day for 5 d after daily administration of leptin (3 mg per kg, intraperitoneal).

Analysis of metabolic phenotype. 3-month-old male mice were acclimated in metabolic chambers (TSE Systems) for 4 d before the start of the recordings. Mice were continuously recorded for 3 d with the following measurements being taken every 30 min: water intake, food intake, ambulatory activity (in X and Z axes) and gas exchange (O_2 and CO_2) (using the TSE LabMaster system). VO_2, VCO_2 and energy expenditure were calculated according to the manufacturer's guidelines (PhenoMaster Software, TSE Systems). Body composition was measured using magnetic resonance imaging (EchoMRI).

Electron microscopy. Under deep anesthesia, 3-month-old male mice were killed by perfusion (4% paraformaldehyde (wt/vol), 0.1% glutaraldehyde (vol/vol), and 15% picric acid (vol/vol) in phosphate buffer (PB)), and their brains were processed for immunolabeling for electron microscopy studies. Ultrathin sections were cut on a Leica Ultra-Microtome, collected on Formvar-coated single-slot grids and analyzed with a Tecnai 12 Biotwin electron microscope (FEI). The electron microscopy photographs (×11,500) were used to measure astrocytic coverage and the numbers of synapses on perikaryal membrane of POMC and unlabeled neurons. The analysis of synapse number was performed in an unbiased fashion as described elsewhere[3,20]. The analysis of the astrocytic coverage was performed as described previously[5,6]. All investigators were blinded to the experimental groups during the entire procedure.

Electrophysiology. *Gfap-Lepr*$^{+/+}$ and *Gfap-Lepr*$^{-/-}$ mice (4-week-old male) labeled with the *Pomc-GFP* or *Npy-hrGFP* were killed at the beginning of the dark cycle, and the ARC was sliced into 250 µm slices (two per mouse), containing the *Pomc-GFP* or *Npy-hrGFP* cells. Slices were then incubated with artificial cerebrospinal fluid at 35 °C for 4 h. After stabilization in artificial cerebrospinal fluid, slices were transferred to the recording chamber for recording mIPSCs and mEPSCs as described previously[3,21].

Immunohistochemistry. 3-month-old male mice were anesthetized and transcardially perfused with 0.9% saline (wt/vol) containing heparin (10 mg l^{-1}) followed by fixative (4% paraformaldehyde, 15% picric acid, 0.1% glutaraldehyde in 0.1 M PB). Brains were collected and post-fixed overnight before coronal sections were taken at every 50 µm. Sections were washed and then treated with 1% H_2O_2 (vol/vol) for 15 min to remove endogenous peroxidase activity. After washing and blocking with 2% normal horse serum (vol/vol), sections were incubated with primary antibodies (antibody to mouse GFAP, 1:1,000 for 2 h at 20–22 °C, Sigma, G3893; antibody to rabbit c-fos, 1:2,000 for overnight at 20–22 °C, Millipore, ABE457; antibody to chicken GFP, 1:2,000 for overnight at 20–22 °C, Abcam, ab13970; antibody to mouse NeuN, 1:1,000 for overnight at 20–22 °C, Millipore, MAB377; antibody to rabbit Iba-1, 1:2,000 for overnight at 20–22 °C, Wako, 019-19741). The following day, sections were extensively washed and incubated in biotinylated secondary antibody to rabbit, ABC reagent and diaminobenzidine (DAB) substrate (Vector Laboratories). Crystal violet staining was performed to detect cell nuclei. Immunofluorescence was performed with a combination of Alexa Fluor 488–labeled secondary antibodies to rabbit, chicken or mouse (1:500 for 1 h at 20–22 °C, Invitrogen, #A21206, #A11039, #A21202) or Alexa Fluor 594–labeled secondary antibodies to rabbit or mouse (1:500 for 1 h at 20–22 °C, Invitrogen, #A21207, #A21203). Representative images were selected from experiments that had been repeated at least three times.

Quantification of astrocyte number and projections. For the quantitative evaluation of astrocytes, six sections throughout the arcuate nucleus per animal were analyzed. Astrocytes were detected by DAB-based immunohistochemistry with GFAP antibody followed by crystal violet staining to identify their nuclei. Images were captured with a 40× objective using a digital camera and analyzed using ImageJ software. Cells were counted according to the optical disector technique[3]. The number of primary projections was determined for each GFAP-positive cell that was included entirely in the field of analysis and Sholl's analysis[7] was performed to assess differences in the extension of glial processes as described previously[22].

Detection of *Lepr* mRNA in astrocyte (*in situ* hybridization). To verify our animal model with specific deletion of leptin receptor expression in astrocytes, we combined *in situ* hybridization with immunohistochemistry using astrocyte-specific leptin receptor knockout (*Gfap-Lepr*$^{-/-}$) mice and their control mice (*Gfap-Lepr*$^{+/+}$). To this end, we designed leptin receptor–specific riboprobes to specifically recognize mRNA region corresponding to *Lepr*-delta exon 17 allele (NM_146146, NCBI GenBank). The riboprobes were labeled with S^{35} and purified with a spin RNA column (Roche Diagnostics). Brain tissues from *Gfap-Lepr*$^{-/-}$ and control animals were quickly removed, frozen in liquid nitrogen, coronally sectioned at 20-µm thickness using a cryostat, and stored in −80 °C until use. First, we performed radioactive *in situ* hybridization using the S^{35}-labeled riboprobes as above following the protocol reported previously[23]. Briefly, sections were fixed with 3% paraformaldehyde solution, acetylated (2.7 ml of triethanolamine and 0.5 ml of acetic anhydride in 200 ml of RNase-free water), dehydrated through a series of alcohols, and then hybridized with the riboprobes at 52 °C for overnight. The next day, the sections were washed through regular washing steps[23], and were ready for immunohistochemistry to visualize astrocyte using a GFAP antibody as a molecular marker for astrocyte. After the washing steps, the sections were incubated with a milk blocking buffer (3% fat-free milk, 0.3% Triton X-100 in 0.1 M PB) at 20–22 °C for 30 min. Next, a series of antibody incubations was performed as following: antibody to mouse GFAP (1:1,000 for 2 h

at 20–22 °C, Sigma), antibody to rabbit POMC (1:1,000 for overnight at 20–22 °C, Phoenix pharmaceuticals, H-029-30) and Alexa 594–conjugated antibody to mouse IgG (1:250 dilution in 0.1 M PB, Invitrogen, #A21203) at 20–22 °C for 1 h. Regular 0.1 M PB washing was performed between antibody incubations. The sections were then finally subjected for emulsion autoradiography and further microscopy.

Astrocyte primary culture. Mice at postnatal day 3 were killed by decapitation and the hypothalamus was collected in DMEM F12 (Gibco) plus 1% antibiotics-antimycotics (Gibco). The hypothalamus was dissociated and the suspension was centrifuged for 7 min at 201*g*. The pellet was resuspended with DMEM F12 plus 10% fetal bovine serum (Gibco by Life Technologies) and 1% antibiotics-antimycotics. This media was used to seed and grow cells in 25-cm^3 culture treated flasks at 37 °C and 5% CO_2. The media was changed every 2 d until the cells reached the desired confluence. Once confluence was reached, between days 7 and 9 *in vitro*, the flasks were place in an incubator shaker at 280 r.p.m. at 37 °C overnight. After shaking, the cells were then washed with phosphate-buffered saline (Gibco), trypsinized and resuspended in DMEM F12 plus 10% fetal bovine serum and 1% antibiotics-antimycotics. The suspension was centrifuged for 5 min at 266*g*. After cell counting, the cells were seeded in poly-L-lysine hydrobromide–coated (10 μg ml^{-1}, Sigma-Aldrich) six-well plates at a concentration of 130,000 cells per well. The cells were grown for 24 h in DMEM F12 containing 10% fetal bovine serum and 1% antibiotics-antimycotics and then treated with 4-hydroxytamoxifen at a concentration of 1 μM or vehicle during 3 consecutive days. Cells were then collected for RNA extraction and PCR analysis.

RT-PCR and ribosome profiling. RNA was extracted using QIAGEN RNeasy Micro Kit (#74004). cDNA was synthetized using QIAGEN Whole Transcriptome Kit (#207043). RT-PCR was performed in a Roche 480 LightCycler using Taqman probes (*Agrp* (Mm00475829_g1); *Leprb* (Mm01262069_m1); *NeuN* (Mm01248771_m1); *s100β* (Mm00485897_m1)). To validate the deletion of exon 17 in cording region of the leptin receptor gene, we designed specific primer set (forward, 5′-TCG ACA AGC AGC AGA ATG AC -3′; reverse, 5′-CTG CTG GGA CCA TCT CAT C-3′) and performed RT-PCR with tamoxifen-treated astrocyte primary cells.

Translating ribosome affinity purification (TRAP) was conducted in homogenate samples of hippocampus and hypothalamus obtained from *AldH-EGFP-L10a* mice, which express green fluorescent protein in the ribosomes of $AldH^+$ cells and mice with *loxP*-flanked *Rpl22* (ribosome protein subunit 22)[24] crossed with the *Agrp-cre* line, which express Rpl22 and HA proteins in ribosomes of AgRP neurons, thereby allowing for the immunoprecipitation of polysomes directly from astrocytes and AgRP neurons[24]. TRAP methods were conducted as previously published[25–27]. After RNA isolation, we obtained approximately 10–25 ng of RNA per sample. RT-PCR was performed as described above.

Statistical analyses. Statistical analyses were performed by use of Prism 6.0 software (GraphPad). Data distribution was assumed to be normal, but this was not formally tested. No statistical methods were used to predetermine sample sizes, but our sample sizes are similar to those reported in previous publication[16,28]. All analyses were performed in a blinded manner. No randomization was used to assign experimental groups or to collect data but mice and cells were assigned to specific experimental groups without bias. Unpaired *t* test was performed to analyze significance between two experimental groups. Two-way ANOVA analysis was performed to detect interaction between treatment and genotype. Two-way repeated-measures ANOVA analysis was used to detect interaction between time and genotype. Significance was taken at $P < 0.05$.

A **Supplementary Methods checklist** is available.

18. McMinn, J.E. *et al. Am. J. Physiol. Endocrinol. Metab.* **289**, E403–E411 (2005).
19. Patterson, C.M., Leshan, R.L., Jones, J.C. & Myers, M.G. Jr. *Brain Res.* **1378**, 18–28 (2011).
20. Diano, S. *et al. Nat. Neurosci.* **9**, 381–388 (2006).
21. Caron, E., Sachot, C., Prevot, V. & Bouret, S.G. *J. Comp. Neurol.* **518**, 459–476 (2010).
22. Del Cerro, S., Garcia-Estrada, J. & Garcia-Segura, L.M. *Glia* **14**, 65–71 (1995).
23. Jeong, J.K., Chen, Z., Tremere, L.A. & Pinaud, R. *J. Vis. Exp.* **42**, 2102 (2010).
24. Sanz, E. *et al. Proc. Natl. Acad. Sci. USA* **106**, 13939–13944 (2009).
25. Heiman, M. *et al. Cell* **135**, 738–748 (2008).
26. Doyle, J.P. *et al. Cell* **135**, 749–762 (2008).
27. Dougherty, J.D., Schmidt, E.F., Nakajima, M. & Heintz, N. *Nucleic Acids Res.* **38**, 4218–4230 (2010).
28. Dietrich, M.O. *et al. Nat. Neurosci.* **15**, 1108–1110 (2012).

doi:10.1038/nn.3725